

Table 1 Summary of patient data

Patient no./age (year)/sex	Tumor location	Tumor diameter (cm)	Tumor character	Number of previous TACE	Number of TACE of A1	Conditions of A1	Site of S1 supplying RIPA branch	Iodized oil distribution in S1	RIPA supply to S1 before TACE of A1
1/69/M	SP	2.5	Recurrence	2	2	Occluded	First Br	SP (dorsal)	N/A
2/62/F	SP	0.8, 0.8, 0.8	Recurrence	2	2	Occluded	First Br First Br of Ant Br.	SP (dorsal)	Yes
3/64/M	CP	1.3	Recurrence	10	2	Attenuated	First Br	SP (dorsal), CP (entire)	No
4/62/F	SP	1.4	Recurrence	1	1	Attenuated	First Br	SP (dorsal)	N/A
5/80/M	SP	2.2	Recurrence	3	2	Occluded	First Br of Ant Br	SP (dorsal)	No
6/49/F	SP	1.2	Recurrence	4	1	Occluded	First Br of Post Br	SP (dorsal)	Yes
7/71/M	SP	2.6	New	3	2	Attenuated	First Br of Ant Br	SP (dorsal)	N/A
8/76/M	SP	1.4	Recurrence	4	2	Occluded	First Br of Ant Br	SP (dorsal)	N/A
9/65/M	SP	2.7, 2.8	New	11	0	Attenuated	First Br First Br of Ant Br	SP (dorsal)	No
10/82/F	S7	1	Recurrence	2	0	Intact	First Br	SP (dorsal), CP (entire)	N/A
11/77/M	S7	2	New	2	1	Occluded	First Br	CP (posterocaudal)	N/A
12/67/M	SP	2	New	6	0	Intact	First Br	SP (dorsal)	Yes
13/76/F	SP	1.3	Recurrence	6	1	Occluded	First Br of Ant Br	SP (dorsal)	No

M Male, *F* female, *SP* Spiegel lobe, *CP* caudate process, *A1* caudate artery, *S1* caudate lobe, *Br* branch, *N/A* not available, *Ant* anterior, *Post* posterior, *S7* segment 7

Tumor location

Eleven patients had one to three HCC lesions (total 14 HCC lesions; range and mean diameter 0.8–2.7 and 1.6 ± 0.7 cm, respectively) in the caudate lobe. Eight patients had recurrent tumors after TACE of the caudate artery, and three had a newly developed tumor. Thirteen tumors were located in the SP and one was located in the CP, of which nine were located at the liver surface and five were embedded in the liver parenchyma. The remaining two patients had a tumor in the posterior segment of the right lobe of the liver near the caudate lobe, 1 and 2 cm in diameter, respectively.

Condition of the previously embolized caudate arteries

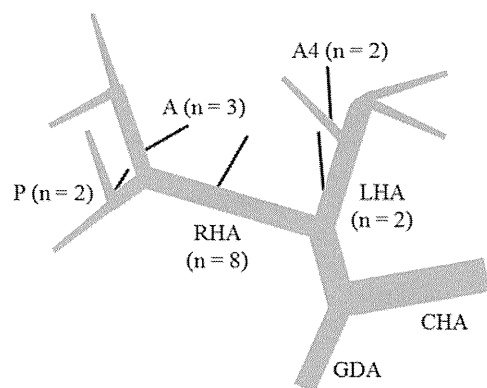
In total, 17 caudate arteries derived from the right hepatic artery ($n = 8$), left hepatic artery ($n = 2$), medial segmental artery of the left hepatic artery ($n = 2$), anterior segmental artery of the right hepatic artery ($n = 3$), or

posterior segmental artery of the right hepatic artery ($n = 2$) had already been embolized in 15 TACE procedures in 10 patients (Fig. 2). An angiography performed when the blood supply to the caudate lobe from the RIPA was demonstrated revealed that 15 caudate arteries were occluded and two were severely attenuated. In two of three patients who did not undergo TACE of the caudate artery, the caudate artery arising from the right hepatic artery was intact. In the remaining patient, the caudate artery arising from the right hepatic artery was attenuated by repeat TACE sessions through the right hepatic artery, although the caudate artery was not selectively embolized.

Selective TACE of the proximal RIPA branches

The embolized branches of the RIPA are summarized in Fig. 3.

In three patients, embolization of the RIPA had been performed during the treatment course before disclosure of the blood supply to the caudate lobe from the RIPA. In one



CHA common hepatic artery, *GDA* gastrooduodenal artery, *LHA* left hepatic artery, *RHA* right hepatic artery, *A4* medial segmental artery of the left hepatic artery, *A* anterior segmental artery of the right hepatic artery, *P* posterior segmental artery of the right hepatic artery

Fig. 2 Schematic presentation of the previously embolized caudate arteries

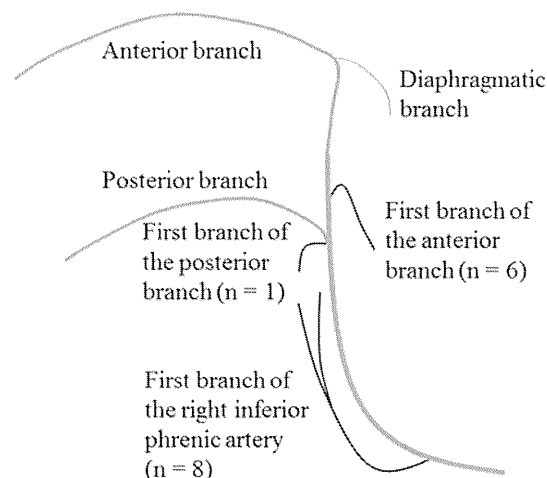


Fig. 3 Schematic presentation of the embolized proximal right inferior phrenic artery (RIPA) branches

patient, a small amount of gelatin sponge particles was injected from the posterior branch of the RIPA during the initial TACE for HCC in the caudate lobe to block equivocal staining near the tumor (Fig. 4). In the other two patients, selective TACE of the posterior branch of the RIPA was performed to treat another tumor in the posterior segment of the right lobe of the liver (Fig. 5).

Selective TACE was performed at the first branch derived from the proximate portion of the RIPA ($n = 8$), the first branch of the anterior branch ($n = 6$), and the first branch of the posterior branch ($n = 1$). In two patients, both the first branch of the RIPA and the first branch of the anterior branch were embolized (Fig. 4). In four patients who underwent CT or CBCT to confirm blood supply to the caudate lobe from the RIPA, the first branch of the right

Fig. 4 A 62-year-old woman with hepatocellular carcinoma (HCC) in the caudate process (CP) of the caudate lobe. **a** Angiogram of the caudate artery arising from the right hepatic artery shows a tumor stain. Transcatheter arterial chemoembolization (TACE) was performed at this point. **b** Angiogram of the RIPA obtained before TACE shows hepatogram of the Spiegel lobe (SP) (arrowheads). A small amount of gelatin sponge particles was injected through the posterior branch of the RIPA to block the equivocal staining (arrow). **c** Unenhanced computed tomography (CT) obtained 1 week after TACE shows iodized oil distribution into the tumor and the SP. **d** The tumor recurred at the SP (not shown), and the second TACE was performed through the caudate artery arising from the left hepatic artery. **e** Angiogram of the RIPA obtained before the second TACE shows attenuation of the posterior branch and there is no tumor staining. Hepatogram of the SP becomes clearer. **f** Unenhanced CT obtained 1 week after the second TACE shows iodized oil distribution into the anterior part of the SP. **g** The tumor recurred and the third TACE was performed. The two previously embolized caudate arteries were occluded (not shown). Angiogram of the RIPA shows a small tumor stain (arrow). **h** Coronal view of slab-maximum intensity projection (MIP) image of the RIPA created from cone-beam CT (CBCT) during angiography of the RIPA shows three tumors (arrows) and hepatogram of the SP. **i** The first branch was selected and TACE was performed; arrow indicates tumor. **j** The first branch derived from the anterior branch was also selected and TACE was performed. **k** Unenhanced CT obtained 1 week after the third TACE shows iodized oil distribution into the posterior part of the SP. Iodized oil is also distributed into the anterior segment of the right lobe of the liver because of additional TACE for another tumor

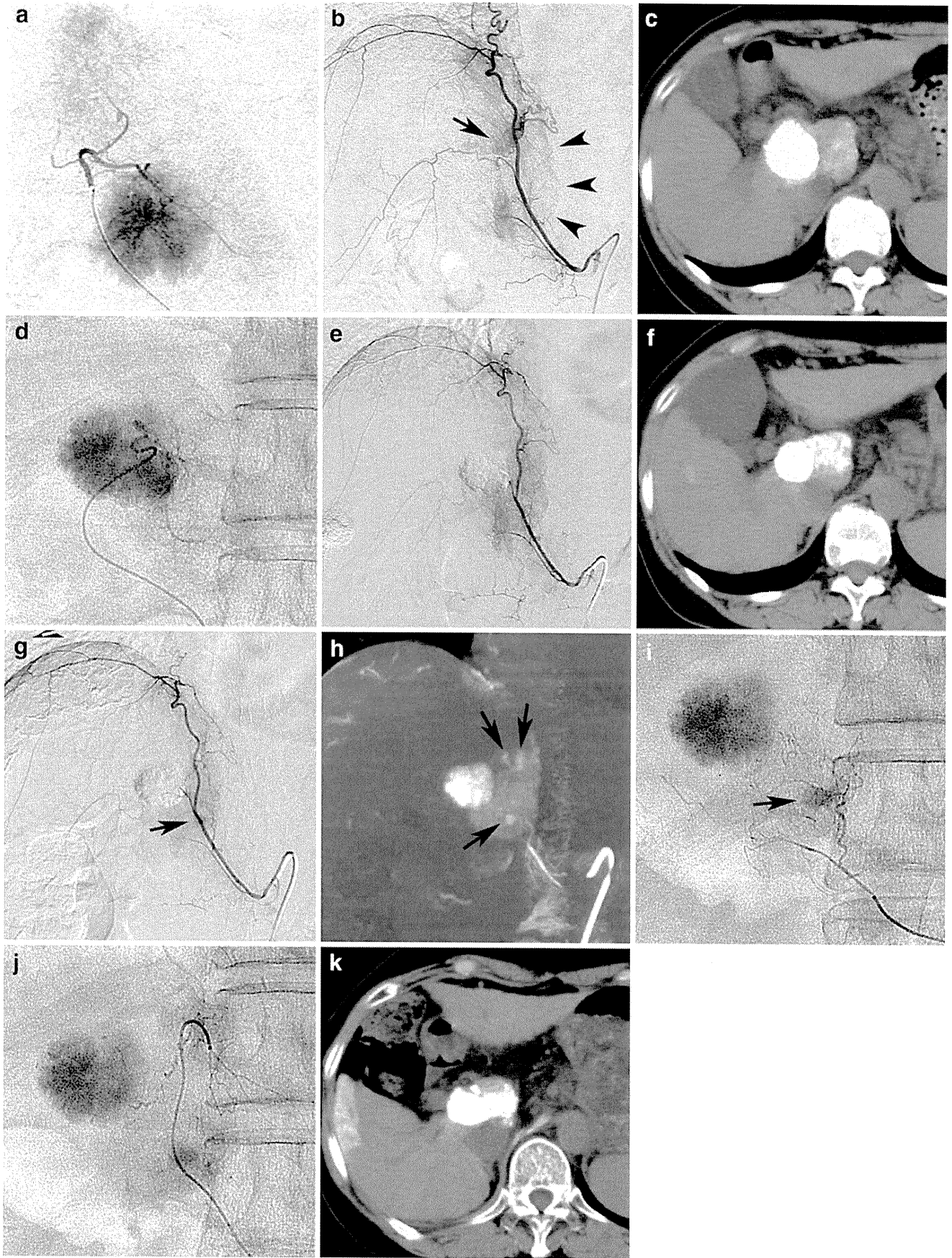
IPA ran behind the inferior vena cava and delivered small branches that directly entered the liver through the posterior surface of the liver, subsequently spreading into the caudate lobe and posterior segment of the right lobe of the liver, in addition to supplying blood to the right adrenal gland (Fig. 5).

Findings of serial RIPA angiography

Of seven patients who had undergone serial RIPA angiography during the previous TACE procedures, the characteristic hepatogram of the SP was retrospectively demonstrated in three patients on the initial angiograms obtained before TACE of the caudate artery (Fig. 4). In the remaining four patients, hepatogram of the SP was not demonstrated on the initial RIPA angiograms, only becoming apparent on the RIPA angiogram obtained after TACE of the caudate artery (Fig. 5).

Iodized oil distribution after TACE of the proximal RIPA branches

Iodized oil was accumulated in the target tumors in or near the caudate lobe in all patients, and its distribution was also demonstrated in one to two subsegments of the caudate lobe. It was distributed into the SP in 10 patients, mainly the posterior part (Fig. 4), into the posterocaudal part of the CP in one patient, and into almost the whole SP or posterior part of the SP and almost the whole CP in the



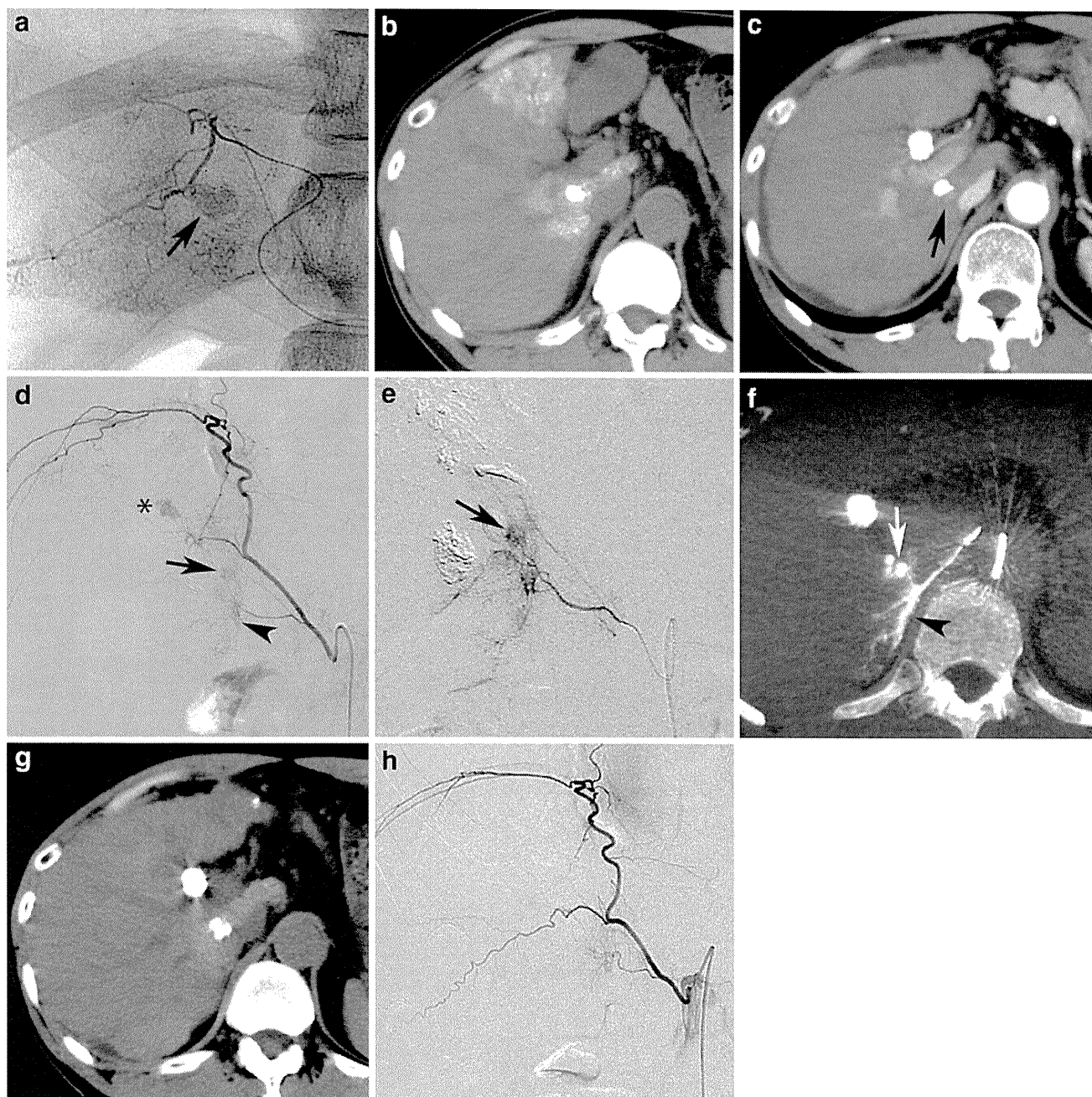


Fig. 5 A 64-year-old man with HCC in the CP of the caudate lobe. **a** The caudate artery arising from the right hepatic artery was selected and TACE was performed; *arrow* indicates tumor. **b** Unenhanced CT obtained 1 week after TACE shows iodized oil distribution into the caudate process (CP) and SP. Iodized oil is also distributed into the medial segment during TACE for another HCC in the medial segment. **c** Arterial phase CT image obtained 16 months after TACE shows local recurrence (*arrow*). Another tumor with accumulation of iodized oil is also seen in the right hepatic hilum. **d** Angiogram of the RIPA shows a tumor stain (*arrow*) and hepatogram of the SP (*arrowhead*). Another tumor supplied by the posterior branch attenuated by the previous TACE is also seen (*asterisk*). The

previously embolized caudate artery was attenuated and did not feed the recurrent tumor (not shown). **e** Angiogram of the first branch shows tumor staining (*arrow*). **f** Axial view of slab-MIP image created from CBCT during angiography of the branch shows that three branches enter into the liver through the posterior surface of the liver and that one branch reaches the recurrent tumor (*arrow*); *arrowhead* indicates staining of the right adrenal gland. TACE was performed at this point. **g** Unenhanced CT obtained 1 week after TACE shows iodized oil distribution into both the CP and SP, almost equal to the area where iodized oil is distributed from the caudate artery. **h** Angiography of the RIPA obtained before the initial TACE does not show any hepatograms of the SP

remaining two patients (Fig. 5). In all 10 patients who had undergone TACE of the caudate artery, the area of iodized oil distribution into the caudate lobe after TACE of the branches of the RIPA was complementary (Fig. 4) or almost equal (Fig. 5) to that after the previous TACE of the caudate artery.

Discussion

Since the liver is suspended from the diaphragm by the coronary and triangular ligaments, the branches of the RIPA are in direct contact with the liver at the bare area [1–3]. Therefore, HCC located near the diaphragm frequently receives its blood supply from the IPA [4, 5, 10, 11], especially when the hepatic arterial circulation is interrupted by repeated TACE or the placement of a catheter for infusion chemotherapy. The perirenal space is anatomically connected with the bare area on the right side [12]. Therefore, the right renal capsular artery also distributes into the bare area [13], and the RIPA and the right renal capsular artery are potentially connected each other [14]. In addition, the right or left gastric, dorsal pancreatic, and right adrenal arteries are possible collateral vessels that serve to supply the caudate lobe of the liver [7, 10].

In the present study, all previously embolized caudate arteries were found to be damaged in all cases where blood supply to the caudate lobe from the proximal branches of the RIPA was demonstrated. This supports the theory that attenuation of the caudate artery by TACE was the main cause of the RIPA parasitization to the caudate lobe, in particular to the SP. However, the RIPA parasitization to the SP was also observed in three patients who had no histories of TACE of the caudate artery. In two of these three patients, the caudate artery was seen to be intact on the angiogram when the blood supply from the RIPA to the SP was demonstrated. Of the seven patients who had undergone angiography of the RIPA prior to TACE of the caudate artery, the characteristic hepatogram of the SP was retrospectively demonstrated in three patients. We speculate that the RIPA originally supplied the SP in at least five of the patients (38.5%) in our study, leading to the supposition that the RIPA is a potential pathway supplying the SP. In addition, in some cases the SP may originally be fed by a dual source of arterial blood, namely, from both the caudate arteries and the RIPA and, in other cases, by arterial blood from the RIPA alone.

In our patients, iodized oil injected through the proximal branches of the RIPA was mainly distributed into the dorsal part of the SP. This result suggests that the dorsal part of the SP may likely receive blood from the proximal RIPA branches because the SP protrudes from the liver and is located adjacent to the bare area. However, depending on

individual variations in hepatic arterial circulation and damage by previous TACE, the proximal RIPA branches may also supply the CP. In addition, the absence of iodized oil accumulation in some part of the SP, mainly in the anterior portion, may also indicate the presence of other blood sources as well as the RIPA.

In the literature, the first branch of the RIPA is called the middle suprarenal branch or superior adrenal branch, and it usually supplies the perirenal adipose tissues and right adrenal gland [1, 2]. In our study, this branch was the most common blood source from the RIPA to the SP. Anastomosis between this branch and the caudate artery on angiography has also been demonstrated [14]. CT or CBCT obtained during the TACE procedure in our series showed that the first branch directly entered the liver through the liver surface and delivered small branches toward the caudate lobe and posterior segment of the right lobe of the liver. Because of a direct connection between the RIPA branches and liver, the vascular territory of the caudate artery may be replaced by the RIPA when the caudate artery is damaged by previous TACE. Change in the blood source supplying the caudate lobe may make it difficult to treat HCC lesions in the caudate lobe by TACE [6, 7].

TACE of the IPA may cause several complications, such as shoulder pain, pleural effusion, basal atelectasis and, infrequently, systemic embolization [15, 16]. Weakness of the diaphragm may also occur, especially when nonselective TACE of the IPA is performed [17]. To prevent these complications, it is important to select the tumor-feeding branch derived from the IPA. Therefore, interventional radiologists should become thoroughly familiar with the possible branches of the RIPA supplying the caudate lobe in order to attempt a selective TACE procedure. CBCT during the TACE procedure may be helpful to prevent nontarget embolization and to determine whether equivocal staining on the RIPA angiography is a tumor [18].

There are several limitations to our study. First, the necessity of TACE through the RIPA was mainly based on angiographic findings. When angiograms of the RIPA did not show obvious tumor staining in or near the caudate lobe, TACE was not performed. Second, RIPA angiography was not routinely performed when tumor staining in or near the caudate lobe was clearly depicted on the hepatic angiogram. Therefore, blood supply to the caudate lobe from the RIPA might have been overlooked in some cases. Third, we focused on the vascular territories of the proximal RIPA branches. We are well aware that the distal branches, such as the diaphragmatic branch of the RIPA, frequently supply the recurrent tumor in the PC as well as the neighboring hepatic branches. In such cases, however, branches of the RIPA supplying the PC were not well identified because both the hepatic arterial branches and RIPA were simultaneously embolized without having

performed selective CT or CBCT. Therefore, these cases were excluded from our study. Finally, embolization of the RIPA had previously been performed in three patients prior to the demonstration of RIPA parasitization to the caudate lobe. However, we speculated that the RIPA branches potentially able to supply the caudate lobe might not be damaged by selective TACE at the distal level or mild blockage using gelatin sponge particles alone.

Conclusion

The proximal branches of the RIPA mainly supply the SP, especially when the caudate arteries are damaged by previous TACE procedures. However, in some cases, the SP may originally receive the arterial blood from the RIPA. The first branch of the RIPA is the most common blood source to the SP, in particular to the dorsal part. This information may be useful when performing selective TACE for tumors in the SP in order to prevent complications related to nonselective TACE of the RIPA.

References

- Loukas M, Hullett J, Wagner T. Clinical anatomy of the inferior phrenic artery. *Clin Anat*. 2005;18:357–65.
- Duprat G, Charansangavej S, Wallace S, Carrasco H. Inferior phrenic artery embolization in the treatment of hepatic neoplasms. *Acta Radiol*. 1998;29:427–9.
- Gwon DI, Ko GY, Yoon HK, Sung KB, Lee JM, Ryu SJ, et al. Inferior phrenic artery: anatomy, variations, pathologic conditions, and interventional management. *Radiographics*. 2007;27:687–705.
- Kim HC, Chung JW, Lee W, Jae HJ, Park JH. Recognizing extrahepatic collateral vessels that supply hepatocellular carcinoma to avoid complications of transcatheter arterial chemoembolization. *Radiographics*. 2005;25:S25–39.
- Miyayama S, Matsui O, Taki K, Minami T, Ryu Y, Ito C, et al. Extrahepatic blood supply to hepatocellular carcinoma: angiographic demonstration and transcatheter arterial chemoembolization. *Cardiovasc Interv Radiol*. 2006;29:39–48.
- Yoon CJ, Chung JW, Cho BH, Jae HJ, Kang SG, Kim HC, et al. Hepatocellular carcinoma in the caudate lobe of the liver: angiographic analysis of tumor-feeding arteries according to subsegmental location. *J Vasc Interv Radiol*. 2008;19:1543–50.
- Miyayama S, Yamashiro M, Yoshie Y, Nakashima Y, Ikeno H, Orito N, et al. Hepatocellular carcinoma in the caudate lobe of the liver: variations of its feeding branches on angiography. *Jpn J Radiol*. 2010;28:555–62.
- Miyayama S, Yamashiro M, Yoshie Y, Okuda M, Nakashima Y, Ikeno H, et al. Inferior phrenic arteries: angiographic anatomy, variations, and catheterization techniques for transcatheter arterial chemoembolization. *Jpn J Radiol*. 2010;28:502–11.
- Kumon M. Anatomy of the caudate lobe with special reference to portal vein and bile duct (in Japanese). *Acta Hepatol Jpn*. 1985;26:1193–9.
- Miyayama S, Yamashiro M, Hattori Y, Orito N, Matsui K, Tsuji K, et al. Angiographic evaluation of feeding arteries of hepatocellular carcinoma in the caudate lobe of the liver. *Cardiovasc Interv Radiol*. 2010 [Epub ahead of print].
- Chung JW, Park JH, Han JK, Choi BI, Kim TK, Han MC. Transcatheter oily chemoembolization of the inferior phrenic artery in hepatocellular carcinoma: the safety and potential therapeutic role. *J Vasc Interv Radiol*. 1998;9:495–500.
- Lim JH, Kim B, Auh YH. Anatomical communications of the perirenal space. *Br J Radiol*. 1998;71:450–6.
- Miyayama S, Yamashiro M, Okuda M, Yoshie Y, Nakashima Y, Ikeno H, et al. The march of extrahepatic collaterals: analysis of blood supply to hepatocellular carcinoma located in the bare area of the liver after chemoembolization. *Cardiovasc Interv Radiol*. 2010;33:513–22.
- Miyayama S, Yamashiro M, Okuda M, Aburano H, Shigenari N, Morinaga K, et al. Anastomosis between the hepatic artery and the extrahepatic collateral or between extrahepatic collaterals: observation on angiography. *J Med Imaging Radiat Oncol*. 2009;53:271–82.
- Tajima T, Honda H, Kuroiwa T, Yabuuchi H, Okafuji T, Yoshimitsu K, et al. Pulmonary complications after hepatic artery chemoembolization or infusion via the inferior phrenic artery for primary liver cancer. *J Vasc Interv Radiol*. 2002;13:893–900.
- Matsumoto K, Nojiri J, Takase Y, Egashira Y, Azuma S, Kato A, et al. Cerebral lipiodol embolism: a complication of transcatheter arterial chemoembolization for hepatocellular carcinoma. *Cardiovasc Interv Radiol*. 2007;30:512–4.
- Lee DH, Chung JW, Kim HC, Jae HJ, Yoon CJ, Kang SG, et al. Development of diaphragmatic weakness after transcatheter arterial chemoembolization of the right inferior phrenic artery: frequency and determinant factors. *J Vasc Interv Radiol*. 2009;20:484–9.
- Miyayama S, Yamashiro M, Hattori Y, Orito N, Matsui K, Tsuji K, et al. Efficacy of cone-beam computed tomography during transcatheter arterial chemoembolization for hepatocellular carcinoma. *Jpn J Radiol*. 2011;29:371–7.

Comparison of local control effects of superselective transcatheter arterial chemoembolization using epirubicin plus mitomycin C and miriplatin for hepatocellular carcinoma

Shiro Miyayama · Masashi Yamashiro · Yoshihiro Shibata ·
Masahiro Hashimoto · Miki Yoshida · Kazunobu Tsuji ·
Fumihito Toshima · Osamu Matsui

Received: 7 September 2011 / Accepted: 5 December 2011
© Japan Radiological Society 2012

Abstract

Purpose To compare local control effects of superselective transcatheter arterial chemoembolization (TACE) using epirubicin (EPI) plus mitomycin C (M) and miriplatin (MPT) for hepatocellular carcinoma (HCC).

Materials and methods One-hundred and twenty-nine HCCs treated with superselective TACE were divided into three groups according to the type of anticancer drug; EPI-M-TACE ($n = 51$), MPT-TACE ($n = 21$), and MPT-I-TACE (MPT emulsion) ($n = 57$). Local recurrence, patterns of recurrence (intratumoral recurrence; IR), and follow-up angiograms were evaluated.

Results Mean tumor diameter and follow-up period for the EPI-M-TACE, MPT-TACE, and MPT-I-TACE groups were 16.9 mm and 15.5 months, 20.7 mm and 12.0 months, and 18.8 mm and 9.6 months, respectively. Local recurrence for the EPI-M-TACE, MPT-TACE, and MPT-I-TACE groups at 5, 10, and 15 months was 6.1, 47.6, and 40.1%, 23.5, 67.3, and 63.9%, and 26.2, 75.4, and 72.9%, respectively. IR for the EPI-M-TACE, MPT-TACE, and MPT-I-TACE groups was 23.1, 71.4, and 71.0%, respectively. Local recurrence

and IR in the EPI-M-TACE group were significantly less than those in the MPT-TACE and MPT-I-TACE groups. Follow-up angiograms revealed less arterial damage in the MPT-TACE and MPT-I-TACE groups.

Conclusion Superselective TACE using MPT resulted in very frequent local recurrence, in particular IR, despite less arterial damage.

Keywords Hepatocellular carcinoma · Transcatheter arterial chemoembolization · Miriplatin · Local recurrence

Introduction

Transcatheter arterial chemoembolization (TACE) is an effective therapeutic option for inoperable hepatocellular carcinoma (HCC) [1–4]. With advances in microcatheter and guidewire technology, the tumor-feeding branch can be selected in almost all patients and local control effects of TACE have been improved [2–4]. It is generally believed that the antitumoral effects of superselective TACE depend mainly on the ischemic effects of the embolic materials, and the importance of anticancer drugs is uncertain.

The anticancer drug miriplatin (MPT; Miripla; Dainippon Sumitomo, Osaka, Japan) is a lipophilic platinum complex [5, 6]. It has been developed as a new drug for use in transcatheter arterial infusion (TAI) for HCC [7]. Recently, it has also been used in TACE [8], however, the therapeutic effects of MPT in TACE have not been established.

Thus, the purpose of this study was to retrospectively evaluate the local control effects of superselective TACE for HCC using MPT compared with that using epirubicin (EPI; Farmorubicin; Pfizer, Tokyo, Japan) plus mitomycin C (M; Mitomycin; Kyowa Hakko Kirin, Tokyo, Japan).

S. Miyayama (✉) · M. Yamashiro · Y. Shibata ·
M. Hashimoto · M. Yoshida · K. Tsuji · F. Toshima
Department of Diagnostic Radiology, Fukuiken Saiseikai
Hospital, 7-1 Funabashi, Wadanaka-cho, Fukui 918-8503, Japan
e-mail: s-miyayama@fukui.saiseikai.or.jp

O. Matsui
Department of Radiology, Kanazawa University Graduate
School of Medical Science, 13-1 Takara-machi,
Kanazawa 920-8641, Japan

Materials and methods

Our institutional review board approved the use of MPT in TACE and written informed consent was obtained for each patient before the procedure. This was a retrospective study using imaging data and clinical records with no change in patient care. Institutional review board approval is not required at our institution for this type of study.

Patients

We defined superselective TACE as TACE performed at the more distal level of the subsegmental artery of the hepatic artery, including ultraselective TACE (TACE at the most distal level of the subsubsegmental artery) and subsegmental TACE (TACE at the subsegmental artery). Between October 2009 and October 2010, we treated 129 newly developed HCC lesions smaller than 6 cm in diameter in 87 patients (46 men and 41 women, mean age \pm standard deviation, 73.0 ± 7.8 years; range 48–88 years) with superselective TACE. Tumor diameter ranged from 7 to 54 mm (18.4 ± 9.5 mm).

Diagnosis of HCC was established on the basis of findings from computed tomography (CT) imaging and/or magnetic resonance imaging (MRI)—characteristic homogenous or mosaic-like nodular enhancement on the arterial phase and wash out on delayed phase images, in addition to nodular staining on angiography and/or CT during hepatic arteriography (CTHA), and nodular perfusion defect on CT during arterial portography (CTAP) obtained using cone-beam CT (CBCT).

The patients were divided into three groups according to the type of anticancer drug used in the TACE procedure. Table 1 shows the patient characteristics for each group. Fifty-one tumors of 33 patients were treated with TACE using a mixture of iodized oil (Lipiodol; Andre Guerbet, Aulnay-sous-Bois, France), contrast material (370 mg I/ml iopamidol, Iopamiron 370; Bayer Schering Pharma, Osaka, Japan), EPI, and M (EPI-M-TACE

group). Twenty-one tumors of 15 patients were treated with TACE using an MPT-iodized oil suspension (miriplatin/LPD) (MPT-TACE group). Fifty-seven tumors of 39 patients were treated with TACE using a mixture of MPT/LPD and contrast material (MPT-I-TACE group). EPI-M-TACE was performed between October 2009 and April 2010, MPT-TACE was performed between January 2010 and June 2010, and MPT-I-TACE was performed between July 2010 and October 2010. Between January 2010 and April 2010, both EPI-M-TACE and MPT-TACE were performed. Selection of anticancer drugs was not randomized and was decided on the basis of the physician's preference.

TACE procedure

All TACE procedures were performed superselectively by use of a microcatheter with a tip less than 2F (Carnelian PIXIE; Tokai Medical Products, Kasugai, Japan; Progreat Σ ; Terumo, Tokyo, Japan) through a 4F catheter. In the EPI-M-TACE group, 2–5 ml iodized oil, a contrast material of 1/3 iodized oil, and anticancer drugs (10–30 mg EPI and 2–6 mg M) were mixed by pumping 10 times by use of a three-way stopcock valve and two 5 to 10-ml syringes. In the MPT-TACE group, one vial of MPT (70 mg) was dissolved in 4 ml iodized oil (MPT/LPD). In the MPT-I-TACE group, a contrast material of 1/2 MPT/LPD was mixed in to create an emulsion by the same technique as described above. In both the MPT-TACE and MPT-I-TACE groups, the maximum dose of MPT was limited to 140 mg. The total amount of iodized oil was determined on the basis of the tumor size in each group. After injection of a mixture of iodized oil and anticancer drugs, gelatin sponge particles (Gelpart; Nippon Kayaku, Tokyo, Japan; approximately 0.5 or 0.2 mm in diameter), crushed by pumping 20 or 50 times by use of a three-way stopcock valve and two 2.5-ml syringes, were injected to completely obstruct the tumor-feeding branch in all three groups.

Table 1 Patient characteristics of each group

	EPI-M-TACE group	MPT-TACE group	MPT-I-TACE group
No. of patients	33	15	39
Male/female	16/17	6/9	24/15
Age	71.9 ± 7.9	75.3 ± 4.7	72.0 ± 8.5
Etiology (HCV/HBV/others)	22/5/6	11/4/0	24/7/8
Child–Pugh class (A/B/C)	16/12/5	12/3/0	24/14/1
T factor (T1/T2/T3) ^a	12/16/5	4/8/3	17/16/6
AFP level (ng/ml)	39.7 ± 57.7	445.8 ± 1856.2	238.5 ± 1100.9
PIVKA-II level (mAU/ml)	445.8 ± 1856.2	807.7 ± 1864.4	204.4 ± 506.9
No. of previous TACE sessions	1.4 ± 1.9	1.3 ± 1.8	1.7 ± 2.3

HCV hepatitis C virus, HBV hepatitis B virus, AFP alpha-fetoprotein, PIVKA-II protein induced in vitamin K absence II

^a Definitions of TMN stage proposed by the Liver Cancer Study Group of Japan

Follow-up

Unenhanced CT was performed 1 week after TACE for all patients to check for iodized oil accumulation in the target tumor.

All patients were followed-up and dynamic CT and/or MRI were performed every 2–3 months after the TACE procedures to investigate tumor recurrence. Local recurrence was judged when an early enhancing tumor without iodized oil accumulation was observed in or adjacent to the tumor and/or confirmed by follow-up angiography, CBCTHA, and CBCTAP. Local recurrence was also classified into two patterns; intratumoral recurrence (IR) and peritumoral recurrence (PR) (Fig. 1) [4]. IR was defined as viable tumor correspondence to a defect in which iodized oil had previously been accumulated. PR was defined as a tumor adjacent to an iodized oil accumulated tumor without a defect.

Follow-up angiography and additional TACE for the recurrent tumor were performed if possible. The conditions of previously embolized branches were classified into three grades; reopened, attenuated, and occluded. Development of arteriportal shunts related to previous TACE was also evaluated.

Statistical analysis

Statistical comparison of patient age, tumor diameter, number of the embolized arterial branches, and duration of

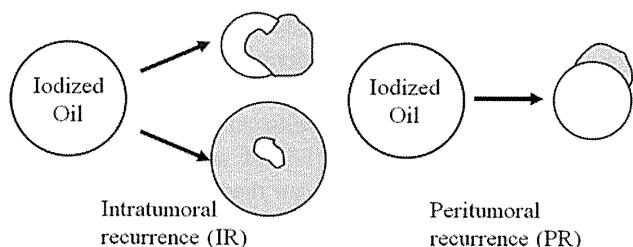


Fig. 1 Schematic representation of intratumoral and peritumoral recurrence. Intratumoral recurrence (IR) was defined as viable tumor correspondence to a defect in which iodized oil had previously been accumulated. Peritumoral recurrence (PR) was defined as a tumor adjacent to an iodized oil accumulated tumor without a defect

Table 2 Summary of each group

	EPI-M-TACE group	MPT-TACE group	MPT-I-TACE group
No. of tumors	51	21	57
Tumor diameter (mm)	16.9 ± 9.1	20.7 ± 11.3	18.8 ± 9.1
No. of embolized branches	1.8 ± 0.6	1.4 ± 0.7	1.6 ± 0.9
No. of subsegmental TACE (%)	7 (13.7)	4 (19.0)	8 (14.0)
Follow-up period (mo)	15.5 ± 4.7	12.0 ± 4.1	9.6 ± 3.1
Tumor recurrence (%)	13 (25.5)	14 (66.7)	31 (54.4)
Time to recurrence (mo)	9.6 ± 4.1	6.0 ± 3.4	5.2 ± 3.0
No. of IR (%)	3 (23.1)	10 (71.4)	22 (71.0)

IR intratumoral recurrence

follow-up periods was performed by one-factor analysis of variance (ANOVA). If statistically significant differences among the three groups were observed, Tukey–Kramer tests were also performed. The gender, etiology of the chronic liver disease, Child–Pugh class, T-factor, TACE levels, IR, and incidence of occlusion or attenuation of the embolized branches of each group were compared by use of the χ^2 test. Incidence of cumulative local recurrence was calculated by use of the Kaplan–Meier method and compared. The generalized Wilcoxon test was used to evaluate significant differences in each group. Values of $P < 0.05$ were considered significant. Statistical calculations were performed by use of StatView version 5.0 software (SAS, Cary, NC, USA).

Results

Results are summarized in the Table 2.

Patient characteristics, tumor diameter, levels of TACE, number of embolized branches, and follow-up periods

There were no significant differences in gender, age, etiology of chronic liver disease, Child–Pugh class, and T-factor among the three groups ($P = 0.2970, 0.3125, 0.4102, 0.0890, \text{ and } 0.8346$, respectively). There were also no significant differences in tumor diameter, levels of the TACE procedure, or number of the embolized arterial branches among the three groups ($P = 0.2857, 0.8292, \text{ and } 0.3157$, respectively). The follow-up period for the EPI-M-TACE group was significantly longer than those for the MPT-TACE and MPT-I-TACE groups ($P < 0.01 \text{ and } 0.001$, respectively). There was also a significant difference in the follow-up periods between the MPT-TACE and MPT-I-TACE groups ($P < 0.05$).

Local tumor recurrence

Dense iodized oil accumulation compared with the surrounding liver parenchyma was observed for all target

tumors in each group on CT performed 1 week after TACE (Figs. 2, 3).

Local recurrence was observed in 13/51 tumors (25.5%) in the EPI-M-TACE group (Fig. 2), 14/21 tumors (66.7%) in the MPT-TACE group, and 31/57 tumors (54.4%) in the MPT-I-TACE group (Fig. 3). Four of 13 tumors (30.8%) in the EPI-M-TACE group, 4/14 tumors (28.6%) in the MPT-TACE group, and 5/21 tumors (23.8%) in the MPT-I-TACE group recurred after subsegmental TACE. Cumulative local recurrence in the EPI-M-TACE, MPT-TACE, and MPT-I-TACE groups after 5, 10, and 15 months was 6.1, 47.6, and 40.1%, 23.5, 67.3, and 63.9%, and 26.2, 75.4, and 72.9%, respectively. Local recurrence in the EPI-M-TACE group was significantly less than that in the MPT-TACE and MPT-I-TACE groups ($P < 0.0001$ and 0.0001 , respectively) (Fig. 4).

Among recurrent tumors, IR in the EPI-M-TACE, MPT-TACE, and MPT-I-TACE groups was 23.1% (3/13), 71.4% (10/14), and 71.0% (22/31), respectively. IR in the EPI-M-TACE group was significantly lower than that in the MPT-TACE and MPT-I-TACE groups ($P < 0.05$ and 0.05 , respectively).

Follow-up angiography findings

Follow-up angiography was performed for 11/13 recurrent tumors in the EPI-M-TACE group, 9/14 in the MPT-TACE group, and 28/31 in the MPT-I-TACE group. In the EPI-M-TACE group, the embolized branch was attenuated in eight tumors (72.7%). In three tumors (27.3%), the embolized branch was occluded and the neighboring hepatic branch or extrahepatic collateral vessel supplied the recurrent tumor (Fig. 2). In addition, arteriportal shunts in the previously embolized area developed in four tumors (36.4%) (Fig. 2). In the MPT-TACE group, all embolized branches were reopened. In the MPT-I-TACE group, the embolized branch was reopened in 19 tumors (67.9%) (Fig. 3) and attenuated in nine (32.1%). Occlusion or attenuation of the embolized branches in the EPI-M-TACE group was significantly higher than that in the MPT-TACE and MPT-I-TACE groups ($P < 0.001$ and 0.001 , respectively). Arteriportal shunts were not observed in either the MPT-TACE group or the MPT-I-TACE group.

Discussion

TACE is an effective therapeutic options for inoperable HCC [1–4]. To enhance the therapeutic effect and reduce complications associated with TACE, superselective TACE using a microcatheter has become a standard TACE technique for small HCC throughout the world [2–4].

A single anticancer drug, or a combination of several, for example doxorubicin, EPI, M, and cisplatin, have been used in TACE; however, the importance of anticancer drugs in superselective TACE is still unknown. In randomized control studies, there was no evidence that TACE was more effective than transcatheter arterial embolization (TAE) [9, 10]. Kawai et al. [10] reported that the serum alpha-fetoprotein level decreased to a significantly greater extent in the group that received doxorubicin than in the group that did not, although survival was not significantly different between TAE with and without doxorubicin. This result suggested that doxorubicin had some favorable additional effect in TACE. Malagari et al. [11] reported that local recurrence after TACE using doxorubicin-loaded microspheres was significantly lower than after TAE using microspheres, although 1-year survival was no different between the two groups because of the short follow-up. They mentioned that the rationale for addition of a chemotherapeutic agent(s) in TACE is based on the assumption that chemotherapeutics augment the antitumoral action of ischemia, counteracting the stimulation of neoangiogenesis resulting from hypoxia due to embolization [11].

The most effective and least toxic regime in TACE has not yet been established. Several authors have reported that TACE using cisplatin resulted in better overall survival than TACE with doxorubicin or EPI [12–14]. However, cisplatin has severe side effects, including thrombocytopenia, hepatic failure, renal failure, and hypersensitivity reactions [15]. In addition, pre and post-hydration is required to prevent renal damage. MPT is a lipophilic platinum complex and 1,2-diaminocyclohexane platinum(II) dichloride, the active platinum compound binding to the nuclear DNA of tumor cells causing cytotoxicity, is gradually released from MPT/LPD accumulated in the tumor [5–8]. Therefore, MPT can theoretically reduce the adverse effects of platinum and does not require additional hydration. Okusaka et al. [7] reported good results with TAI using MPT/LPD for HCC, and recently it has also been used in TACE, because addition of embolic materials may result in more favorable antitumor effects than TAI [8].

In this study, local tumor recurrence was divided into two patterns; IR and PR [4]. IR may be indicative of incomplete TACE, for example insufficient blockage of the feeding artery or missing of other small feeding branches. PR may be indicative of residual minute tumor growth adjacent to the main mass, fed in part by the portal vein. Therefore, PR usually becomes apparent later than IR after TACE. After introduction of MPT into superselective TACE, we frequently experienced early local tumor recurrence, in particular IR. During the injection of MPT/LPD, the flow through tumor-feeding branches frequently

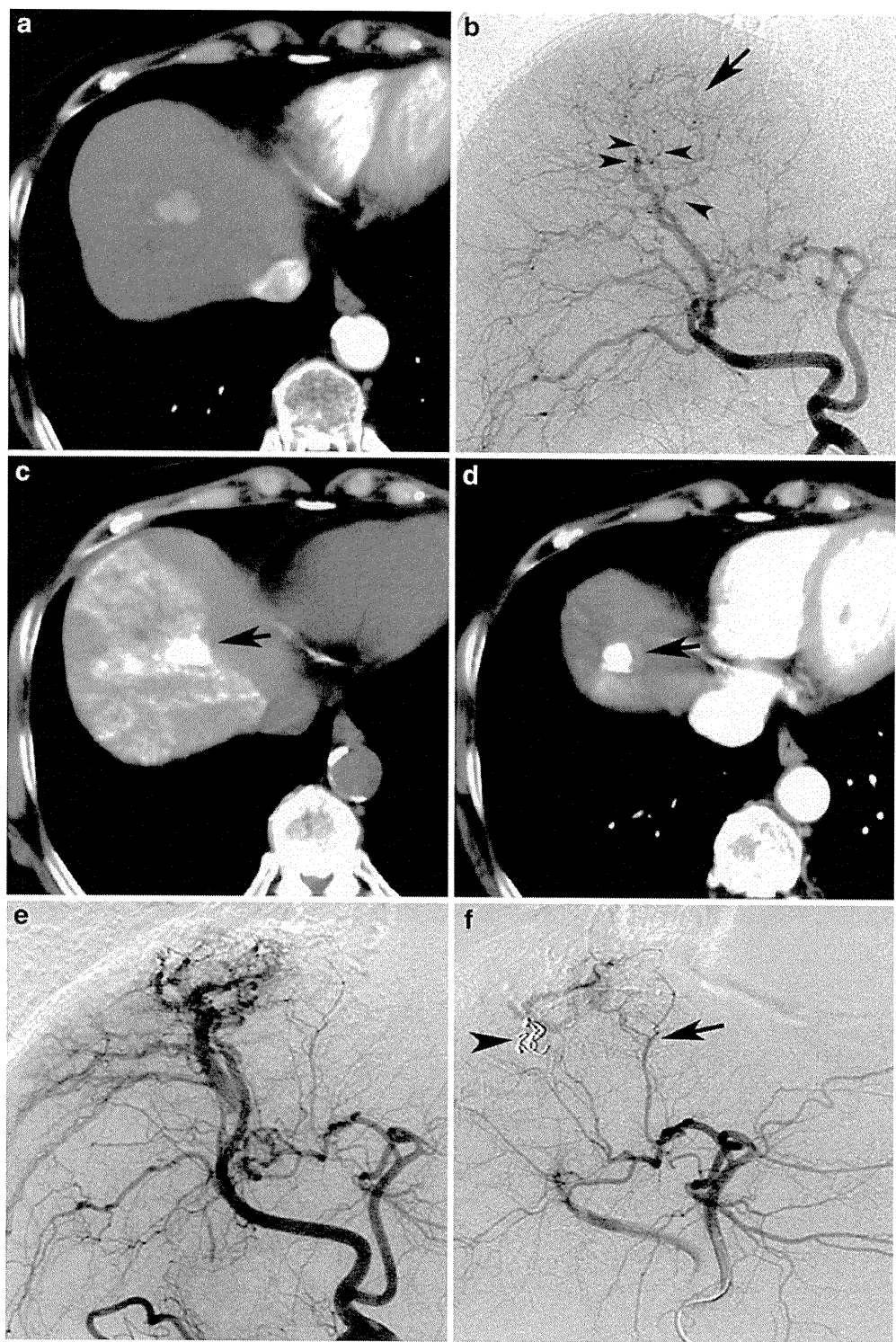


Fig. 2 A case of PR after EPI-M-TACE. **a** Computed tomography (CT) revealed a tumor in segment 8. **b** Common hepatic arteriogram revealed a faint tumor stain (*arrow*). Four branches of the anterior superior subsegmental artery of the right hepatic artery (A8) (*arrowheads*) were selectively embolized. **c** CT performed 1 week after TACE revealed dense iodized oil accumulation in the tumor, however, the left-side safety margin was inadequate (*arrow*). **d** CT performed 11 months after TACE revealed PR at the left side where

an adequate safety margin had not been obtained (*arrow*). **e** Follow-up common hepatic arteriogram showed that the embolized branches were severely attenuated and arterioportal shunts had developed. **f** Left hepatic arteriogram revealed that the recurrent tumor was supplied by a branch of the medial subsegmental artery (*arrow*). Arterioportal shunts were also apparent. The *arrowhead* shows the metallic coils placed in A8 to occlude the arterioportal shunts

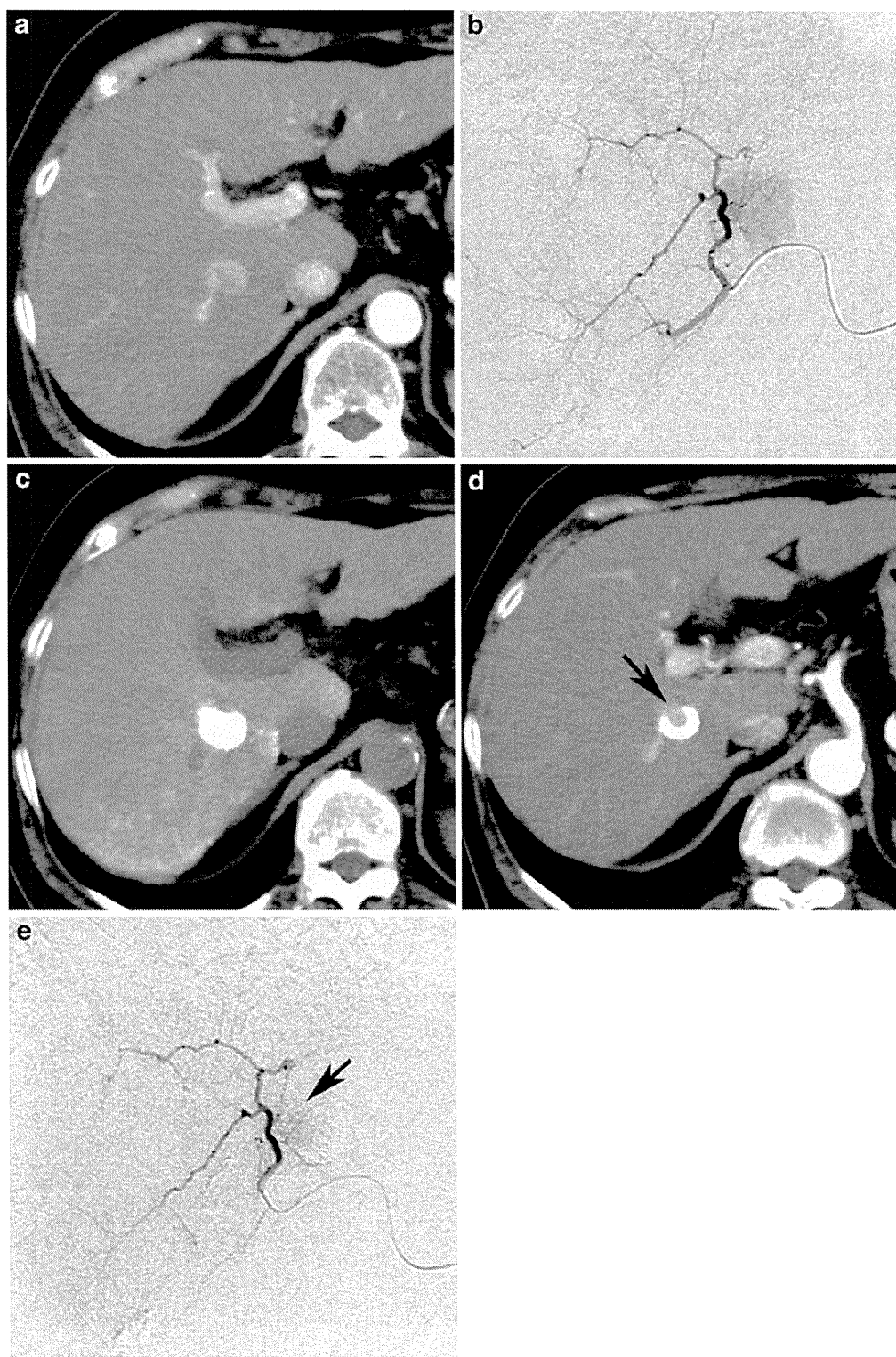


Fig. 3 A case of IR after MPT-I-TACE. **a** CT revealed a small tumor in segment 7. **b** Selective arteriogram of the posterior superior subsegmental artery of the right hepatic artery (A7) revealed a tumor stain. TACE was performed at this point. **c** CT performed 1 week after TACE

showed dense iodized oil accumulation in the tumor. **d** However, CT performed 2 months after TACE revealed IR (*arrow*). **e** Follow-up arteriogram of A7 revealed a tumor stain. In addition, all embolized branches had reopened compared with the initial arteriogram

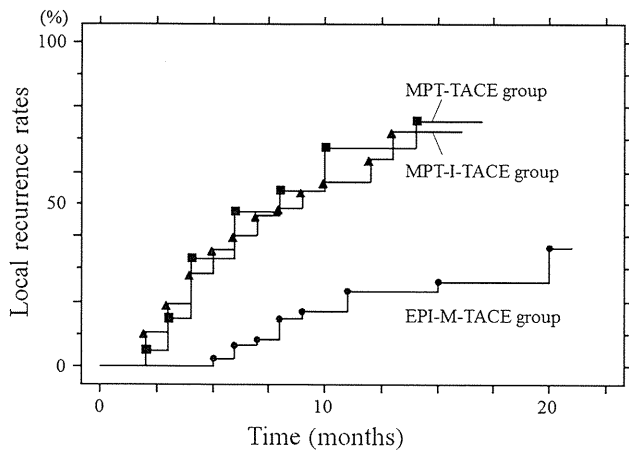


Fig. 4 Plot of cumulative local recurrence in the EPI-M-TACE, MPT-TACE, and MPT-I-TACE groups. Local recurrence in the EPI-M-TACE group was significantly lower than in the MPT-TAE and MPT-I-TACE groups ($P < 0.0001$ and 0.0001 , respectively)

stalled early, because of its high viscosity. In such cases, TACE may have been incomplete because gelatin sponge particles could not be injected adequately. We speculated that the high viscosity of MPT/LPD might be the main cause of IR, and we attempted to reduce the viscosity by mixing contrast material with MPT/LPD to create a water-in-oil (W-O) emulsion, because some authors have reported that hepatic tumor uptake of W-O emulsions was higher than that of pure iodized oil and oil-in-water (O-W) emulsions [16, 17]. However, there were no significant differences in local recurrence between the MPT-I-TACE and MPT-TACE groups and it was still higher than that in the EPI-M-TACE group. Furthermore, the follow-up periods in the MPT-I-TACE group were relatively short, and additional local recurrence, in particular PR, may develop in the future. On the basis of our results, we speculated that the anticancer effect of MPT itself, rather than the type of MPT/LPD, suspension or emulsion, could be the main cause of the very frequent tumor recurrence.

Hamada et al. [6] reported selective distribution and long-term high concentration of platinum in the tumor tissue of the rat liver after injection of MPT/LPD into the hepatic artery. In another experimental study reported by Kishimoto et al. [5], however, only 5.9% of platinum that was initially contained in MPT/LPD was released into saline after 28-days' incubation. This study suggests that the total amount of active platinum released from MPT/LPD is extremely small compared with other hydrophilic anticancer drugs mixed with iodized oil, because these are usually released rapidly from the iodized oil after injection [18, 19].

TACE usually induces arteritis. In addition, development of arterioportal shunts frequently disturbs additional TACE. It is feasible that damage to the hepatic artery by

TACE can be kept to a minimum, to prolong the duration of transcatheter management and avoid reducing the hepatic function reserve [4]. For these reasons, we believe that superselective catheterization is also useful. Follow-up angiograms of the EPI-M-TACE group revealed that all embolized branches were attenuated or occluded. In addition, arterioportal shunts were apparent in 36% of cases. We speculate that superselective EPI-M-TACE severely damages the arteries and this may exaggerate the ischemic effects on tumors. On the other hand, follow-up angiograms after MPT-TACE or MPT-I-TACE showed that almost all embolized branches were reopened and that there were no arterioportal shunts in the embolized areas. This suggests that MPT does not injure the arteries, and that the embolized arteries including the tumor-feeders may recanalize within a few days, owing to absorption of gelatin sponge particles. As a result, the tumor cells that escape exposure to active cytotoxic agents may revive after receiving the restored arterial blood flow. Less damage to the arteries may work as an advantage to preserve hepatic function and to prevent development of extrahepatic collateral pathways to tumors; however, it may also promote tumor recurrence or survival in addition to slow-release of active platinum.

This study has several limitations. First, the study design was not a strict historical control, because between January 2010 and April 2010, both EPI-M-TACE and MPT-TACE were performed and selection of anticancer drugs was not randomized. This could have caused drug selection bias. Second, we know that the objective of TACE is not to achieve local tumor control but to prolong survival. From the results of this study, it could not be determined whether overall survival in the EPI-M-TACE group was superior to that of the MPT-TACE or MPT-I-TACE groups. However, we believe that local control of the tumor may be directly linked to prognosis in patients with inoperable HCC. In addition, it is well known that rapid progression of surviving tumor cells after treatment is rarely observed [20]. Long-term survival of patients in the MPT-TACE or MPT-I-TACE groups is not expected because of very frequent tumor recurrence.

Conclusion

In superselective TACE for HCC, local recurrence in the MPT or MPT-I-TACE groups was significantly higher than in the EPI-M-TACE group. The characteristics of MPT, for example the slow-release of the active platinum compound and less damage to the arteries, may lead to very frequent tumor recurrence, in particular IR, although less arterial damage may work as an advantage to the nontumorous liver.

References

1. Yamada R, Sato M, Kawabata M, Nakatsuka H, Nakamura K, Takashima S. Hepatic artery embolization in 120 patients with unresectable hepatoma. *Radiology*. 1983;148:397–401.
2. Uchida H, Ohishi H, Matsuo N, Nishimine K, Ohue S, Nishimura Y, et al. Transcatheter hepatic segmental arterial embolization using lipiodol mixed with an anticancer drug and Gelfoam particles for hepatocellular carcinoma. *Cardiovasc Intervent Radiol*. 1990;13:140–5.
3. Matsui O, Kadoya M, Yoshikawa J, Gabata T, Arai K, Demachi H, et al. Small hepatocellular carcinoma: treatment with subsegmental transcatheter arterial embolization. *Radiology*. 1993;188:79–83.
4. Miyayama S, Matsui O, Yamashiro M, Ryu Y, Kaito K, Ozaki K, et al. Ultrasensitive transcatheter arterial chemoembolization with a 2-F tip microcatheter for small hepatocellular carcinomas: relationship between local tumor recurrence and visualization of the portal vein with iodized oil. *J Vasc Interv Radiol*. 2007;18:365–76.
5. Kishimoto S, Noguchi T, Yamaoka T, Fukushima S, Takeuchi Y. In vitro release of SM-11355, cis[[(1R, 2R)-1,2-cyclohexanediamine-N,N']bis(myristato)] platinum(II) suspended in lipiodol. *Biol Pharm Bull*. 2000;23:637–40.
6. Hamada M, Baba A, Tsutsumishita Y, Noguchi T, Yamaoka T, Chiba N, et al. Intra-hepatic arterial administration with miriplatin suspended in an oily lymphographic agent inhibits the growth of tumors implanted in rat livers by including platinum-DNA adducts to form and massive apoptosis. *Cancer Chemother Pharmacol*. 2009;64:473–83.
7. Okusaka T, Okada S, Nakanishi T, Fujiyama S, Kubo Y. Phase II trial of intra-arterial chemotherapy using a novel lipophilic platinum derivative (SM-11355) in patients with hepatocellular carcinoma. *Invest New Drugs*. 2004;22:169–76.
8. Ikeda K, Okusaka T, Ikeda M, Morimoto M. Transcatheter arterial chemoembolization with a lipophilic platinum complex SM-11335 (miriplatin hydrate)—safety and efficacy in combination with embolizing agents. *Jpn J Cancer Chemother*. 2010;37:271–5 (in Japanese).
9. Cammà C, Schepis F, Orlando A, Albanese M, Shahied L, Trevisani F, et al. Transarterial chemoembolization for unresectable hepatocellular carcinoma: meta-analysis of randomized controlled trial. *Radiology*. 2002;224:47–54.
10. Kawai S, Okamura J, Ogawa M, Ohashi Y, Tani M, Inoue J, et al. Prospective and randomized clinical trial for the treatment of hepatocellular carcinoma—a comparison of lipiodol-transcatheter arterial embolization with and without adriamycin (first cooperative study). *Cancer Chemother Pharmacol*. 1992;31 Suppl:s1–6.
11. Malagari K, Pomoni M, Kelekis A, Pomoni A, Dourakis S, Spyridopoulos T, et al. Prospective randomized comparison of chemoembolization with doxorubicin-eluting beads and bland embolization with BeadBlock for hepatocellular carcinoma. *Cardiovasc Intervent Radiol*. 2010;33:541–51.
12. Kamada K, Nakanishi T, Kitamoto M, Aikata H, Kawakami Y, Ito K, et al. Long-term prognosis of patients undergoing transcatheter arterial chemoembolization for unresectable hepatocellular carcinoma: comparison of cisplatin lipiodol suspension and doxorubicin hydrochloride emulsion. *J Vasc Interv Radiol*. 2001;12:847–54.
13. Kasai K, Ushio A, Sawara K, Miyamoto Y, Kasai Y, Oikawa K, et al. Transcatheter arterial chemoembolization with a fine-powder formulation of cisplatin for hepatocellular carcinoma. *World J Gastroenterol*. 2010;16:3437–44.
14. Yodono H, Matsuo K, Shinohara A. A retrospective comparative study of epirubicin-lipiodol emulsion and cisplatin-lipiodol suspension for use with transcatheter arterial chemoembolization for treatment of hepatocellular carcinoma. *Anti-Cancer Drugs*. 2011;22:277–82.
15. Kawaoka T, Aikata H, Katamura Y, Takaki S, Waki K, Hiramatsu A, et al. Hypersensitivity reactions to transcatheter chemoembolization with cisplatin and lipiodol suspension for unresectable hepatocellular carcinoma. *J Vasc Interv Radiol*. 2010;21:1219–25.
16. de Baere T, Zhang X, Aubert B, Harry G, Lagrange C, Ropers J, et al. Quantification of tumor uptake of iodized oils and emulsions of iodized oils: experimental study. *Radiology*. 1996;201:731–5.
17. Demachi H, Matsui O, Abo H, Tatsu H. Simulation model based on non-Newtonian mechanics applied to the evaluation of the embolic effect of emulsions of iodized oil and anticancer drug. *Cardiovasc Intervent Radiol*. 2000;23:285–90.
18. Lewis AL, Gonzalez MV, Lloyd AW, Hall B, Tang Y, Willis SL, et al. DC Bead: in vitro characterization of a drug-delivery device for transarterial chemoembolization. *J Vasc Interv Radiol*. 2006;17:335–42.
19. Varela M, Real MI, Burrel M, Forner A, Sala M, Brunet M, et al. Chemoembolization of hepatocellular carcinoma with drug eluting beads: efficacy and doxorubicin pharmacokinetics. *J Hepatol*. 2007;46:474–81.
20. Kojiro M, Sugihara S, Kakizoe S, Nakashima O, Kiyomatsu K. Hepatocellular carcinoma with sarcomatous change: a special reference to the relationship with anticancer therapy. *Cancer Chemother Pharmacol*. 1989;23 Suppl:s4–8.

